Surface properties on magnesium alloy and corrosion behaviour based high-speed wire electrical discharge machine power tubes

Jinkai Xu[1], Kui Xia[1], Zhongxu Lian[1], Linshuai Zhang[1], Huadong Yu[1], Zhanjiang Yu[1], Zhankun Weng[2], Zuobin Wang[2]

[1]*College of Mechanical and Electric Engineering, Changchun University of Science and Technology, Changchun 130022, People's Republic of China*
[2]*International Research Centre for Nano Handling and Manufacturing of China, Changchun University of Science and Technology, Changchun 130022, People's Republic of China*
E-mail: yuhuadong@cust.edu.cn

Published in Micro & Nano Letters; Received on 15th May 2015; Revised on 14th September 2015; Accepted on 16th October 2015

The effect of power tubes on AZ91D magnesium (Mg) alloy was investigated by high-speed wire electrical discharge machine (WEDM-HS). This Letter presented the different surface characteristics and corrosion resistance of the fabricated surface. Chemical composition of the fabricated surface was analysed by energy-dispersive X-ray spectroscopy, and the surface salt water contact angle was also measured in this study. The machined surface evidenced a carbon layer and high hydrophobic property (contact angle between 146° and 150°). The corrosion resistance of the samples machined by the WEDM-HS process was studied in 3.5% NaCl solution through electrochemical impedance spectroscopy. The results have shown that when electrical parameters of the five power tubes were used, the good surface properties of the fabricated surface were obtained with few micropits, and using the higher power tube was helpful to improve the AZ91D corrosion resistance. A handy WEDM-HS technology for treating AZ91D is a useful way to improve the corrosion resistance of the AZ91D Mg alloy.

1. Introduction: Magnesium (Mg) alloy is considered to be the most excellent green engineering material due to its low density and thermal capacity, high specific strength and fast solidification speed properties. Compared with iron and steel, whether in the reserves, scope of application and recycling, it has very obvious advantages, and keeps consumption growing rapidly. These kinds of light-weight materials have become significant materials for aeronautics, automotive and electronic communications industries [1–3]. Nevertheless, the chemical property of Mg is so lively that the alloy surface will form a layer of thin film after immersing in aqueous solution. As a result, porous oxide film on Mg alloy surface has very poor corrosion protection effect for the long term. Therefore, various methods have been explored to improve the corrosion resistance of Mg alloy. Allahkaram *et al.* [4] illustrated that electroless coating was a potential method to increase corrosion resistance performance materials based on their electrochemical measurements. Jia *et al.* [5] demonstrated Mg alloy with microarc oxidation films for corrosion protection and improvement of cytocompatibility. Guo *et al.* [6] used the electrodeposition technique on Mg alloy surface where it showed a higher corrosion resistance. Taltavull *et al.* [7] decreased the corrosion rate of AZ91D after eliminating the top part of the laser-treated surface. Aung and Zhou [8] found that heat treatment of T4 condition significantly affected AZ91D alloy corrosion behaviour. However, to the best of our knowledge, no attempt has been made previously to create a corrosion resistance of films based on Mg and its alloy by an environmentally friendly fabrication strategy, especially using a method that is efficient, and large-area three-dimensional.

High-speed wire electrical discharge machine (WEDM-HS) has become an important part of advanced manufacturing technology due to its high efficiency. Some researchers have reported that the corrosion resistance of metal was improved by electro-discharge machining technology [9–11]. Nevertheless, the surface of Mg is easy to get damaged during the machining process because of the rapid heating and quenching effect, and the damage has a very big effect on the mechanical properties. Anish *et al.* [12] studied the microstructure and element migration for a rough cut surface of pure titanium after WEDM. Pan *et al.* [13] studied the surface damage layer properties of monocrystalline silicon processed by WEDM.

This Letter mainly researches the surface properties of Mg alloy after WEDM-HS cutting. The microstructure of the machined surface was obtained using different operation parameters. Through the micropit to evaluate surface quality, accordingly, the obtained surface displayed high corrosion resistance and stability, and the corrosion behaviour was investigated by electrochemical measurements in NaCl solution. The whole process was facile to operate in a cutting and did not require advanced and complex devices, making this process widely applicable and easy for mass production.

2. Experimental: Experimental material is one of the widely used industrial rolling of AZ91D Mg alloy, and the chemical compositions of the alloys are given in Table 1. The machine used in the experiment was WEDM-HS of Jinma DK7732 type, the working fluid was JR3A emulsion solution, a molybdenum wire-electrode with a diameter of 0.12 mm and the positive polarity machining mode was used in this study. The pulse duration was 6 μs; the pulse interval was 48 μs; and the AZ91D alloy was sliced into 3 mm × 10 mm × 15 mm samples. After that, the fabricated samples were soaked in kerosene for 10 min. Then all the samples were ultrasonically degreased in acetone for 5 min, followed by ultrasonication with ethanol for 5 min, and dried immediately. A specimen was ground successively by using silicon carbide papers (from 600 to 2000 grits) as the substrate.

The microstructure of the samples is described using scanning electron microscope (JSM-6700F). An energy-dispersive X-ray spectrometer was also used for the analysis of the chemical composition of the fabricated surfaces. Hydrophobic property was tested by salt water contact angles (SWCAs) at three different positions of each sample, and the volume of water drop was 5 μl. Retc

Table 1 Composition of AZ91D Mg alloy

Composition	Al	Zn	Mn	Si	Fe	Ni	Mg
weight, %	8.534	0.522	0.208	0.016	0.002	<0.001	remainder

microfriction and wear tester instrument were used to characterise the friction and wear properties of Mg alloy surface, and a 440C stainless steel ball of 4 mm diameter was used as the dual pieces and the friction way was reciprocating friction; all wear tests were conducted at sliding speeds of 0.2 mm/s under normal load 1 N, and the slip amplitude was 5 mm.

Electrochemical tests were performed by CS310 electrochemical workstation. A three-electrode configuration was employed in these tests, the working electrode had an exposed sample area of 0.5 cm^2, a platinum electrode as the counterelectrode and a saturated calomel electrode as the reference electrode. The samples were immersed in the 3.5 wt% NaCl (18 ± 1.5°C) solution without stirring for 10 min, allowed the open-circuit potential of samples to reach the stable values. All experimental chemicals were analytically pure reagents, and the solution was deionised water. The electrochemical impedance spectroscopy (EIS) measurements frequency ranges from 10^{-2} to 10^5 Hz, with a sinusoidal signal perturbation of 10 mV and with seven points per decade.

3. Results and discussion

3.1. Study of surface mechanical properties: It is observed from SEM micrographs of Fig. 1 that WEDM-HS surfaces have irregular topography and typical defects included big etching pits, micro/nanopits, debris particles, pores and microcracks. Fig. 1*a* presents the typical WEDM-HS surface. There was obvious change in surface topography owing to significant change in the electrical parameter of the power tube; Figs. 1*b–f* show WEDM-HS samples treated with one to five power tubes, respectively. Especially, there are many micro/nanopits in the process surface, as shown in Fig. 1*b* for the surface treated with one power tube. Fig. 1*f* presents lots of smooth erosion pits.

In general, when the discharge pulse energy exceed the ultimate strength of materials of the AZ91D surface that lead to materials local damage, the discharge pulse energy can be calculated as

$$W_m = T_e \times I_e \times U_e \tag{1}$$

where T_e is the discharge period, I_e the peak current and U_e is the discharge voltage; the values are indicated in Table 2. According

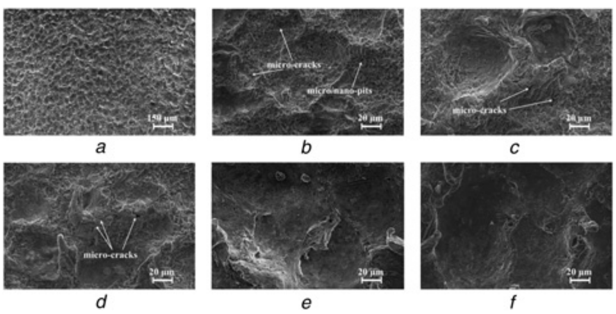

Fig. 1 *SEM micrographs of the WEDM-HS sample treated with different power tube numbers*
a WEDM-HS sample treated with one power tube
b Higher magnification of Fig. 1*a*
c WEDM-HS samples treated with two power tubes
d WEDM-HS samples treated with three power tubes
e WEDM-HS samples treated with four power tubes
f WEDM-HS samples treated with five power tubes

to Figs. 1*b–f*, however, the smoothness of discharge pit increases with the power tube numbers. Mg surface damage mechanism is similar to monocrystalline silicon cut by WEDM. It is just that resistance will rise as the temperatures increase. The main cause of formation of the micro/nanopits is the big heat power density, and the heat power density P can be calculated as follows [13]:

$$P = \frac{I^2 R}{V} = \frac{(j\Delta s)^2(\Delta l\rho/\Delta s)}{\Delta s\Delta l} = \rho j^2 \tag{2}$$

where P is the power density (W/cm^3), I the discharge current (A), R the resistance (Ω), V the conductor volume (cm^3), j the current density (A/cm^2), S the unit area (cm^2), l the unit length (cm) and ρ is the resistance rate (Ω cm). The resistance rate of AZ91D used in the test is 1.535×10^{-5} Ω cm, the current of the lowest discharge energy sample (i.e. treated with one power tube) is 0.46 A (Table 2). According to Fig. 1*b*, the diameter of discharge pits is about 60 μm, so the heat power density is about 4×10^3 W/cm^3. The heat power density of the highest discharge energy sample (i.e. treated with five power tubes) is 1×10^3 W/cm^3. It is obvious that when the heat power density achieves a high value, more micro/nanopits were formed on the surface. Fig. 1*f* shows that, for the highest discharge energy, i.e. treated with five power tubes, during the WEDM process, the machined surface ridge region has sufficient cooling liquid. Therefore the temperature is low, resistance is small and only the ridge region is more easy to form micro/nanopits.

3.2. Corrosion

3.2.1. Energy-dispersive X-ray spectroscope (EDS) analysis: Fig. 2 shows macroscopic views of the AZ91D Mg alloy with various treatments. Fig. 2*a* shows the ground sample. Here, the sample with fabricated WEDM-HS presents black colour (Fig. 2*b*), and it indicates that the surface has new materials in contrast to the substrate. Chemical composition of the WEDM-HS sample was detected through the EDS. Fig. 2*c* presents the EDS analysis and composition of the machined surface. It was found that the carbon and oxygen elements were registered on the surface. In addition, the elements of Mg and aluminium were significantly reduced in contrast to the substrate (Table 1). The EDS for all samples were tested, and the results are similar, so that we use the WEDM-HS sample treated with one power tube as the representative. Other chemical elements of the WEDM-HS surface are listed in Table 3. Therefore, we believe that it is possible to produce a carbon layer during processing. The presence of new materials on the alloy surface may be attributed to oxidation as a result of the high discharge temperature. The water droplets that contain carbon form emulsion solution can be easily gasified and reacted with the melted material [9]. The WEDM-HS surface after being

Table 2 WEDM-HS operating values of current and voltage

Power tube numbers	Current, A	Voltage, V
1	0.46	72
2	0.48	89
3	0.50	91
4	0.55	100
5	0.57	102

doi: 10.1049/mnl.2015.0204

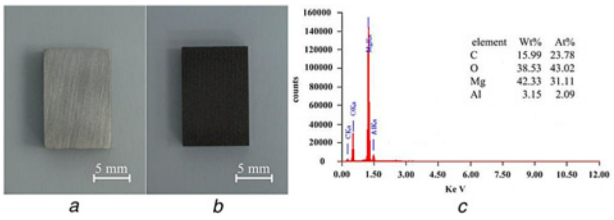

Fig. 2 *Macroscopic image of the AZ91D Mg alloy with various treatments*
a Ground sample
b WEDM-HS sample treated with one power tube
c EDS analysis of surface treated with one power tube

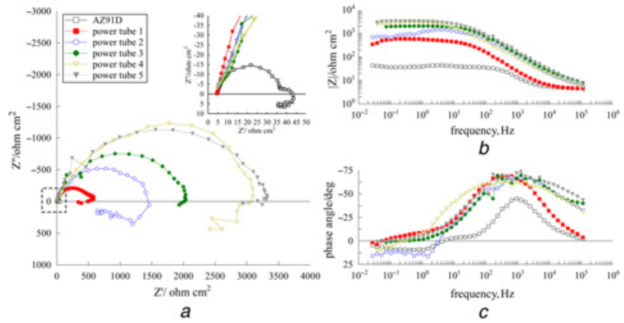

Fig. 3 *EIS spectra of the AZ91D Mg alloy with various treatments in 3.5 wt % NaCl*
a Nyquist plots
b Bode plots of |Z| against frequency
c Bode plots of phase angle against frequency

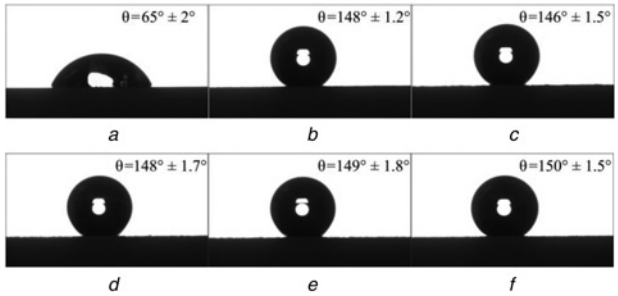

Fig. 4 *SWCAs of fabricated AZ91D samples with different WEDM-HS operation parameters*
a Ground to 2000 grits
b WEDM-HS samples treated with one power tube
c WEDM-HS samples treated with two power tubes
d WEDM-HS samples treated with three power tubes
e WEDM-HS samples treated with four power tubes

kerosene soaked and ultrasonic cleaned still remained the original black colour, which proves that the carbon layer formed on the surface of Mg alloy has excellent adhesion.

3.2.2. Electrochemical impedance spectroscopy: To characterise the corrosion behaviour of the WEDM-HS surface, corrosion tests were completed by using the EIS technique. EIS is a precise and effective electrochemical technique for the evaluation of coating degradation and corrosion kinetic even after short immersion times, which was studied by impedance spectroscopy with a wide frequency range on the electrode system [14]. Accordingly, Fig. 3 shows the EIS spectra of the AZ91D Mg alloy with various treatments in the 3.5 wt% NaCl aqueous solution. Compared with the substrate, the surface impedance of the WEDM-HS samples had an increasing trend. The charge transfer resistance (R_{ct}) value of the highest discharge energy sample (treated with five power tubes) reach up to 3400 Ω cm^2, while that of the substrate is 37 Ω cm^2 (Fig. 3*a*), and the R_{ct} values decrease gradually with decreasing power tube numbers. There are three loops in the Nyquist plot of the AZ91D substrate, including one high-frequency capacitance loop, one medium-frequency capacitance loop and one low-frequency inductance loop. The high-frequency capacitance loop is contributed by the electric double layer at the interface between the substrate and the NaCl solution. The medium-frequency capacitance loop relates to the oxide film generated on the AZ91D surface, and the low-frequency inductance loop is attributed to the initial stage of corrosion [15–17]. Nevertheless, the plot of the WEDM-HS samples has fewer capacitance loops, while the high-frequency capacitance loop is obvious in the plot; especially, the highest discharge energy, i.e. treated with five power tubes. It should be related to the charge transfer resistance of the corrosion process, as the impact of the carbon layer can effectively prevent the formation of loose oxide film and even the initiation of corrosion. Figs. 3*b* and *c* show the Bode plots of the AZ91D Mg alloy with various treatments, the impedance modulus |*Z*| of WEDM-HS fabricated samples is higher than that of the substrate. It is clear that the fabricated samples represent a higher level of impedance than AZ91D, associated with better corrosion resistance performance.

Furthermore, the diverse test results of fabricated samples are attributed to different degrees of surface defects. As the active ions in solution, Cl ion selectively adsorb onto the metal surface that takes place at the defect. A high energy place is susceptible to corrosion where residual microstress and micropits are stored in the surface, in agreement with the literature [18].

3.2.3. Hydrophobic property and corrosion behaviour: Besides, the hydrophobic property of all samples was assessed by SWCAs (3.5 wt% NaCl solution). As shown in Fig. 4, the average SWCA values of all fabricated samples are around 148° ± 2°, and the AZ91D contact angle is 65° (Fig. 4*a*). The hydrophobicity of fabricated Mg alloy surfaces was significantly improved after WEDM-HS. A hydrophobic or super-hydrophobic surface generally brings a high corrosion resistance in a metal surface, and the high corrosion resistance is explained by the air cushion effect. Wang and Kaneko [19] reported that the hydrophobicity can improve the corrosion resistance of the metal surface. For example, Fig. 5 illustrates the effect of surface structure on the hydrophobic property. As the micro/nanostructures of WEDM-HS fabricated surface with a low tension can store a large amount of air, some defects such as

Table 3 Chemical composition of the WEDM-HS surfaces

Power tube numbers	C		O		Mg		Al	
	Wt%	At%	Wt%	At%	Wt%	At%	Wt%	At%
2	31.19	39.85	51.52	49.42	14.28	9.01	3.01	1.71
3	24.75	33.77	44.94	46.03	26.76	18.04	3.54	2.15
4	24.14	33.37	42.36	43.96	30.48	20.82	3.02	1.86
5	31.78	45.50	17.57	18.88	47.84	33.83	2.81	1.79

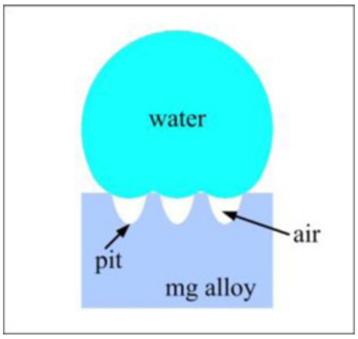

Fig. 5 *Diagrams illustrating the effect of surface structure on the hydrophobic property*

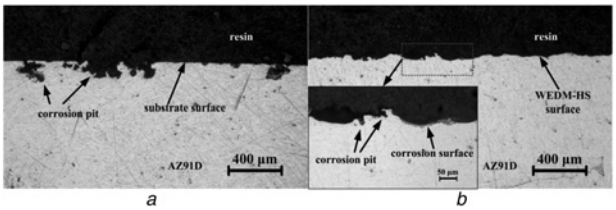

Fig. 6 *Cross-section micrograph of the corroded surface after immersion in 3.5 wt% NaCl aqueous solution for 3 h*
a Substrate
b Highest discharge energy WEDM-HS sample treated with five power tubes

micropit and microcrack are protected by air. Therefore, air cushion will appear and reduce the actual area between the metal surface and the solution. This confirms that the increase of hydrophobicity decreases the wettability of aggressive electrolytes. Therefore, air cushion as a shield prevents the aggressive solution from attacking the material surface.

Fig. 6 presents typical cross-sections of the corroded surfaces of the substrate and the WEDM-HS-fabricated sample after 3 h of immersion in 3.5 wt% NaCl aqueous solution. Fig. 6*a* indicates that the substrate corrosion pits are larger than the fabricated sample which are presented in Fig. 6*b*. This indicates that the corrosion rate of the fabricated sample was decreased in the same environment. The higher corrosion resistance of the fabricated surface than the substrate may be ascribed to less defects in its surface layer. The carbon layer on the substrate surface has a higher electrode potential than the Mg element. Moreover, the carbon layer and air cushion of hydrophobicity act as a barrier or shield to prevent the progress of the corrosion.

To characterise higher application of the WEDM-HS surface, the coefficient of friction (COF) of the Mg alloy surface was tested and different shapes were processed in this Letter. Fig. 7 shows the variation of COF of the alloy surface; however, each COF of fabricated surface was lower than the substrate surface (0.26), and the lowest was 0.146, i.e. WEDM-HS sample treated with one power tube. So it can improve the durability of the Mg alloy surface. WEDM can machine cylindrical surface, concave groove, sharp corner and other special-shaped structures, as shown in Fig. 8, and the motion of the wire electrode in relation to the workpiece is controlled either two or three dimensionally. Hence, many curved surfaces can be machined.

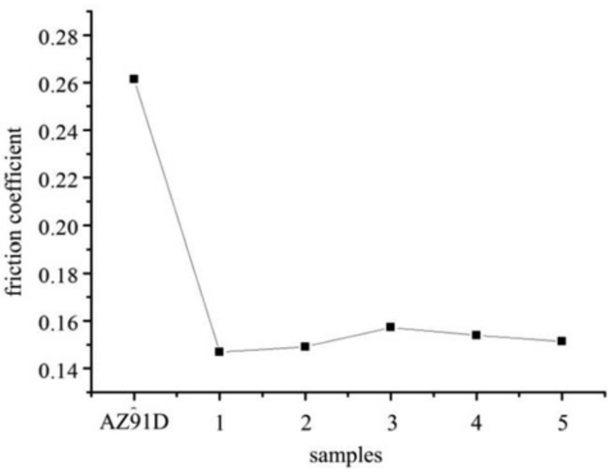

Fig. 7 *Variation of COF of Mg alloy surface (normal load = 1 N; slip amplitude = 5 mm; slid speed = 0.2 mm/s)*
a AZ91D which ground with 2000 grits SiC
b WEDM-HS samples treated with one power tube
c WEDM-HS samples treated with two power tubes
d WEDM-HS samples treated with three power tubes
e WEDM-HS samples treated with four power tubes
f WEDM-HS samples treated with five power tubes

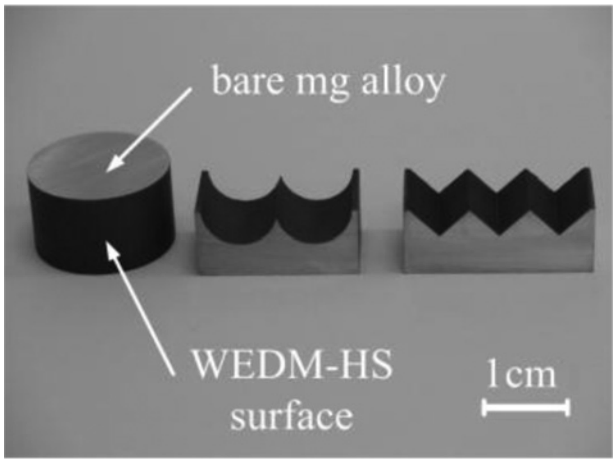

Fig. 8 *Mg alloy of different shapes machined by WEDM-HS*

4. Conclusion: The main defects of the WEDM-HS surface of Mg alloy have big roughness values, numerous micro/nanopits and microcracks. Five power tubes is the key parameter which will lead to the decrease of the micropits and microcracks, and improve the WEDM-HS machined surface quality. Sufficient cooling and appropriate discharge energy had a crucial impact on the quality of the machined surface. The mechanical properties of the Mg alloy could be improved to reduce the superfluous heat transfer to the substrate. A relationship was established between the electric spark machining parameters and the corrosion impedance of Mg alloy surface, and a high power tube was helpful to improve the AZ91D corrosion resistance. The carbon layer and air cushion of hydrophobicity act as a shield to prevent the progress of corrosion.

5. Acknowledgments: The authors acknowledge the support from the National Natural Science Foundation of China (NSFC, grant no. 51275056 and grant no. 51305043).

6. References

[1] Wang F.H., Du K.Q., Zhang W.: 'Progress in research of corrosion and protection of magnesium alloy', *Mater. China*, 2011, **30**, (2), pp. 29–34 (Chinese)
[2] Ding W.G., Fu P.H., Peng L.M., ET AL.: 'Advanced magnesium alloys and their applications in aerospace', *Spacecr. Environ. Eng.*, 2011, **28**, (2), pp. 103–109 (Chinese)

doi: 10.1049/mnl.2015.0204

[3] Li M.C., Hao S.Z., Wen H., ET AL.: 'Surface composite nanostructures of AZ91 magnesium alloy induced by high current pulsed electron beam treatment', *Appl. Surf. Sci.*, 2014, **303**, pp. 350–353
[4] Allahkaram S.R., Zoughi M., Rabizadeh T.: 'Studying the influence of nano-Al_2O_3 particles on morphology and corrosion improvement of Ni–9%P electroless coatings', *Micro Nano Lett.*, 2010, **5**, (5), pp. 262–265
[5] Jia Z.J., Li M., Liu Q., ET AL.: 'Micro-arc oxidization of a novel Mg-1Ca alloy in three alkaline KF electrolytes: Corrosion resistance and cytotoxicity', *Appl. Surf. Sci.*, 2014, **292**, pp. 1030–1039
[6] Guo X.W., Wang S.H., Gong J., ET AL.: 'Characterization of highly corrosion-resistant nanocrystalline Ni coating electrodeposited on Mg–Nd–Zn–Zr alloy from a eutectic-based ionic liquid', *Appl. Surf. Sci.*, 2014, **313**, pp. 711–719
[7] Taltavull C., Torres B., Lopez A.J., ET AL.: 'Corrosion behaviour of laser surface melted magnesium alloy AZ91D', *Mater. Des.*, 2014, **57**, pp. 40–50
[8] Aung N.N., Zhou W.: 'Effect of heat treatment on corrosion and electrochemical behaviour of AZ91D magnesium alloy', *J. Appl. Electrochem.*, 2002, **32**, pp. 1397–1401
[9] Habib S., Farhat G., Tidiane A., ET AL.: 'Effect of electro discharge machining (EDM) on the AISI316L SS white layer microstructure and corrosion resistance', *Int. J. Adv. Manuf. Technol.*, 2013, **65**, pp. 141–153
[10] Sun S.F., Di S.C., Lu P.X., ET AL.: 'Microstructure and properties of metamorphic layer formed on Mg-RE alloy in micro-EDM process', *Acta Metall. Sin.*, 2013, **49**, pp. 251–256 (Chinese)
[11] Yuan F.C., Chow H.M., Lin Y.C., ET AL.: 'Surface modification using semi-sintered electrodes on electrical discharge machining', *Int. J. Adv. Manuf. Technol.*, 2008, **36**, pp. 490–500
[12] Anish K., Vinod K., Jatinder K.: 'Investigation of microstructure and element migration for rough cut surface of pure titanium after WEDM', *Int. J. Microstruct. Mater. Prop.*, 2013, **8**, pp. 343–356
[13] Pan H.J., Liu Z.D., Gao L., ET AL.: 'Study of small holes on monocrystalline silicon cut by WEDM', *Mater. Sci. Semicond. Process.*, 2013, **16**, pp. 385–389
[14] Abdel S.H., Butt D.P.: 'Novel smart stannate based coatings of self-healing functionality for AZ91D magnesium alloy', *Electrochim. Acta*, 2013, **197**, pp. 296–303
[15] Cao C.N., Zhang J.Q.: 'Introduction of electrochemical impedance spectroscopy' (Science Press, Beijing, China, 2002)
[16] Song Y.W., Shan D.Y., Chen R.S., ET AL.: 'Corrosion characterization of Mg–8Li alloy in NaCl solution', *Corros. Sci.*, 2009, **51**, pp. 1087–1094
[17] Baril G., Galicia G., Deslouis C., ET AL.: 'An impedance investigation of the mechanism of pure magnesium corrosion in sodium sulphate solution', *J. Electrochem. Soc.*, 2007, **154**, pp. 108–113
[18] Guang L.S., Zhen Q.G.: 'The Surface, microstructure and corrosion of magnesium alloy AZ31 sheet', *Electrochim. Acta*, 2010, **55**, pp. 4148–4161
[19] Wang R.G., Kaneko J.: 'Hydrophobicity and corrosion resistance of steels coated with PFDS film', *Surf. Eng.*, 2013, **29**, (4), pp. 255–263